Available online at www.sciencedirect.com
SCIENCE DIRECT®
Journal of Chromatography B, 817 (2005) 127–137
JOURNAL OF CHROMATOGRAPHY B
www.elsevier.com/locate/chromb

Dynamic electric field assisted multi-dimensional liquid chromatography of biological samples

T.P. Hennessy[a,*], M. Quaglia[a], O. Kornyšova[b], B.A. Grimes[a], D. Lubda[c], K.K. Unger[a]

[a] *Institut für Anorganische Chemie und Analytische Chemie, Johannes Gutenberg-Universität, Duesbergweg 10-14, D-55099 Mainz, Germany*
[b] *Department of Chemistry, Vytautas Magnus University, Vileikos 8, LT-44404 Kaunas, Lithuania*
[c] *Merck KGaA, Frankfurter Str. 250, D-64293 Darmstadt, Germany*

Received 15 April 2004; accepted 15 October 2004

Abstract

Complex biological samples require very high resolution separation strategies. The platform introduced here capitalises on the hyphenation of liquid chromatographic (LC) and electric potential gradient electrochromatographic multi-dimensional separation genres. First-dimension selectivity is provided by simultaneous size exclusion (SEC) and strong cation exchange (SCX) chromatography modes, while the second dimension comprises reversed phase (RP) characteristics in a dynamic (time-variant) electric field. The time-variant potential gradient with reversal of polarity is applied across the second dimension monolithic capillary throughout the duration of the solvent strength gradient elution. Hence, the platform offers comprehensive on-line sample clean-up (matrix depletion, analyte enrichment), fractionation (first dimention LC), and separation (second dimension LC) with the prospect of altering selectivity via polarity reversal dynamic electric field tuning.

Keywords: Multidimensional liquid chromatography; Size exclusion chromatography; Strong cation exchange chromatography; Reversed phase chromatography; Affinity chromatography; Tailor-made sorbents; Monolithic capillary columns; On-line sample clean-up; Human hemofiltrate; Human plasma; Electrically assisted liquid chromatography; Polarity reversal; Dynamic electric field; Transport mechanism

1. Introduction

Complex biological samples demand separation strategies with very high resolving power. A multitude of sophisticated methodologies is currently available to address the desire for (sufficient) appropriate separation space to accommodate representatively the whole sampled universe from a large universe of a small sample quantity [1–6].

The complexity of biological samples in general, and proteomic questions in particular, have paved the way for multi-dimensional liquid chromatography (MDLC) to be established as a complementary tool to two-dimensional polyacrylamide gel electrophoresis (2D PAGE) among the arsenal of analytical equipment to meet the requirements of the post-genomic era. The assets and drawbacks of many of these platforms have recently been documented [7–11]. The versatility of MDLC approaches is unparalleled as the known facets of selectivity provided by tailor-made sorbents may be combined to a multitude of off-line tandem processing systems [12,13]. The more elaborate on-line arrangements are marginally reduced in their resourcefulness paying tribute only to the requirement of compatibility between the hyphenated dimensions (with respect to column hardware dimensions, selectivity and operational features) [4,14], whereby the most popular two-dimensional sequential combination to date is represented by strong cation exchange (SCX) and reversed phase (RP) selectivity [15]. Automated sample preparation and sample clean-up steps are introduced with increasing frequency to serial analytical separation strategies [16,17]. As a consequence, the development of separation

* Corresponding author. Tel.: +49 6131 3925927/6151 728209; fax: +49 6131 3922710/6151 7294355.
E-mail address: tom.hennessy@ungerversum.de (T.P. Hennessy).

1570-0232/$ – see front matter © 2004 Published by Elsevier B.V.
doi:10.1016/j.jchromb.2004.10.043

strategies associated with a particular analytical goal rather than a specific sample should be a cherished creed for separation scientists [18].

In analogy to gradient elution in pressure-driven high performance liquid chromatography (HPLC), gradient systems for electromigration techniques in general, and capillary electrochromatography (CEC) in particular, materialise to be essential to target complex samples. A variety of different gradient installations have been reported [19–24]. International Union of Pure and Applied Chemistry (IUPAC) recommendations on the terminology for analytical capillary electromigration techniques are available [25]. Despite the fact that theoretical approaches to quantitatively describing and modelling electrokinetic techniques vary significantly in complexity and mass transfer involved [26–29], and moreover general theoretical certainty with respect to mutual interactions of the analysis system's protagonists lacking abundance [30], cross-over applications/techniques emerge with their evolution driven by the quest for separation space and resolution within. Irrespective of their particular individual contribution and in arbitrary sequence the authors are inspired by the following publications [31–34]. For the feasibility study in hand, the data recorded by pressure-driven solvent strength gradients under the influence of an electric field applied across the separation capillary obviously proved most prominent [35].

The initial campaign propagated here is hyphenation of SCX LC with integrated sample clean-up via SEC on a bimodal functionalised chromatographic material in the first dimension and electrically assisted RP LC in the second dimension. While the two-dimensional LC system with integrated sample clean-up is well established [17] the electric field fine-tuning capacity in the second dimension is a novelty to separation science literature. The separation system set-up may be byzantine, but in return offers the total scope of versatility provided by the individual hyphenated analysis machinery to create the novel separation platform. Previously [35,36], electrically assisted LC (in one dimension) was associated with the tag 'selectivity fine-tuning' in particular in the mixed mode operation status. Superimposing two gradients (in one dimension or the second of two dimensions) of thoroughly different origins (pressure-driven solvent strength gradient and electrically-driven voltage gradient with reversal of polarity) defiantly may be associated with 'selectivity tuning' as the result may prompt drastic amendments to the resulting raw-data profiles.

The approach documented in this paper combines the features of reducing sample complexity by adopting the strategy of integrated sample clean-up by simultaneous SEC and SCX via the choice of the bifunctional spherical particle based sorbent in the first dimension and orthogonal, complementary analyte separation by simultaneous two-pronged gradient-driven mass transport through the endcapped RP monolith serving as the second dimension of a potentially comprehensive on-line multi-dimensional separation platform.

2. Experimental

2.1. Samples

Hemofiltrate was generously provided by IPF PharmaCeuticals, Hannover, Germany, while the human plasma was obtained from the DRK (German Red Cross) Frankfurt, Germany from healthy volunteers undergoing routine blood sampling. Blood was collected in sampling tubes, inhibited with citrate and centrifuged prior to screening against HIV and Hepatitis viruses, respectively. Citrate-plasma was pooled from viral-negative blood donors and stored frozen at −80 °C.

2.2. Equipment

A contemporary two-dimensional liquid chromatography platform resembles the backbone of the equipment hyphenated with a state-of-the-art capillary electrophoresis (here, more precisely: electrochromatography) apparatus utilised in the present case to enhance the achievable resolution of the individual separation tools. The entire platform is set up from Agilent Technologies (formerly Hewlett Packard) modules namely the 1100 series system comprising solvent trays, degassers, binary pumps, autosampler, diode-array detector (DAD), instrument control (ChemStation) and the HP^{3D}CE likewise equipped with a DAD. The individual systems are both ChemStation controlled and communication of the individual systems occurs via a remote control cable. Hyphenation of the autonomous dimensions is executed by a T-splitter set to ground potential. The splitter serving the purpose of assimilating the flow between the hyphenated separation dimensions and representing the flow-through electrode generating ground potential to create the potential difference for the application of the (dynamic) electric field with optional reversal of polarity in the second dimension. Column switching and analyte transfer, respectively occur by way of a two-position six-port valve from Rheodyne. All tubing and connectors are PEEK (poly ether ether ketone) from Upchurch Scientific. All presented (electro)chromatograms are recorded by the DAD of the HP^{3D}CE apparatus. A chart of the system is detailed in Fig. 1.

2.3. Columns

All sorbents utilised in these studies are either Merck KGaA, Darmstadt, Germany products or – at the time of manuscript preparation – research specimens from the afore named company.

First dimensional separations are performed on restricted access material (RAM) columns 25 mm × 4 mm length and inner diameter (i.d.) respectively, packed with 25 μm spherical beads with an average pore size of 60 Å (LiChrospher® 60 XDS (SO_3H/Diol) 25 μm). A bimodal surface functionalisation provides diol groups bonded to the outer surface and

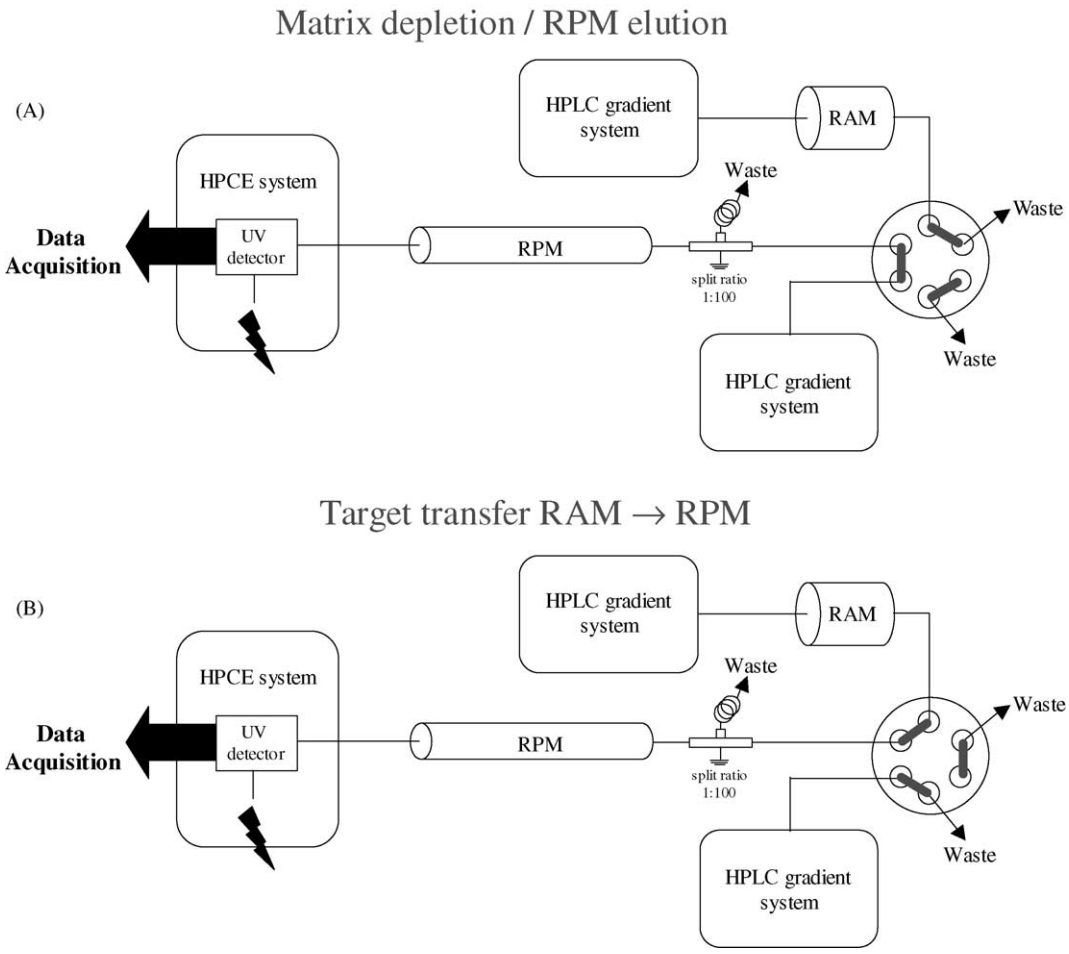

Fig. 1. Chart of the coupled column system hyphenated via a two-position six-port valve. The flow paths for (A) first dimension matrix depletion on the RAM (LiChrospher® 60 XDS (SO_3H/Diol) 25 μm) column and second dimension separation on the RPM (Chromolith® CapRod® RP-18 endcapped 300–0.1 mm) and (B) target transfer from the RAM → RPM. For 1D separations the entire RAM system and for 2D separations the autosampler/injector of the RPM system are bypassed, respectively.

strong cation exchange groups on the inner surface of the particles, respectively [37,38].

The second dimension (electro)chromatographic column is a 300 mm × 0.36 mm (100 μm i.d.) fused silica capillary featuring a silica monolith in the capillary format [39,40] with C-18 modification and endcapping (e) (Chromolith® CapRod® RP-18 endcapped 300–0.1 mm).

Human serum albumin (HSA) depletion is achieved by off-line affinity chromatography.

2.4. Methods

Since the separation platform is created from independent building blocks, the chromatographic methods have to be established individually. The hydrodynamic drive for the first and second dimensions is customised depending on the sorbent [12] and column dimension dependent [41], while the second dimension only is optimised with respect to sample specificity. The latter is likewise true for the application of the polarity reversal electric potential gradient assisted elution albeit the method (voltage) programming occurs on the HP^{3D}CE ChemStation (the two-pronged gradient elution off the second dimension (or sole dimension in the one-dimensional system) is simultaneously provided by two co-operating remote-controlled ChemStations). The obligation of transparency demands presentation of methods, procedures and conditions in separate sections. The first dimension separations of the two-dimensional (2D) systems are discussed in the relevant section (*two-dimensional separations*). Single dimension (1D) separations and second dimension separations in the 2D systems are provided by the same solvent delivery system and mobile phases are hence denoted A″ and B″, respectively. First dimension solvents in the 2D system are specified as A′ and B′, respectively. Off-line mobile phases are designated (non-primed) A and B. Flow-rates are detailed as specified in the methods for the solvent delivery systems and the passive split-resultant flow-rate is given in parentheses [41].

2.4.1. One-dimensional separations

The separations in Fig. 3 are obtained by injection of 10 μl human hemofiltrate in water (10 mg/ml). The solvent

gradient run time is 30 min from A″ (5 mM sodium phosphate pH 7.5) → B″ (70/30, v/v CH_3CN/A″) at a flow-rate of 0.2 ml/min (2.0 μl/min). The prevailing electric fields are established via voltage programming of (a) 0 kV (pure solvent gradient LC), (b) +20 kV, (c) −20 kV, and inaugural (d) +20 kV → −20 kV simultaneously superimposed on the time-variant solvent composition.

Acquisition of the human plasma profiles in Fig. 4 is accomplished by injection of 10 μl diluted sample (1/10, v/v plasma/A″). The solvent gradient run time is 46 min from A″ (water + 0.1% TFA (trifluoroacetic acid)) → B″ (CH_3CN + 0.09% TFA) at a flow-rate of 0.2 ml/min (1.5 μl/min). The voltage program is equivalent to Fig. 3 adjusted to the present solvent gradient run time. Additionally, the full range electric potential difference provided by the $HP^{3D}CE$ instrument is exploited in (e) +30 kV → −30 kV (cf. Fig. 3).

The Fig. 5 plot provides 1D versus 2D LC obtained under identical elution conditions from the Chromolith® CapRod® RP-18 endcapped 300–0.1 mm. The solvent gradient run time is 30 min from A″ (water + 0.1% TFA) → B″ (CH_3CN + 0.09% TFA) at a flow-rate of 0.1 ml/min (1.5 μl/min). Human hemofiltrate injections are 10 μl in A′ (10 mg/ml) in the respective cases.

The 1D separation in Fig. 6 is obtained by injection of 10 μl human hemofiltrate in A′ (10 mg/ml) under the conditions employed in Fig. 3(d) with the exception of the initial flow-rate (prior to flow splitting) being 0.1 ml/min (1.5 μl/min).

The 1D separation in Fig. 7 is recorded under conditions equivalent to those utilised to generate the Fig. 4(e) profile with the exception of the initial flow-rate (prior to flow splitting) being 0.1 ml/min (1.5 μl/min). Human plasma injection is 10 μl diluted sample (1/10, v/v plasma/A′) in the respective cases.

The 1D separation in Fig. 8 is recorded under conditions equivalent to those utilised to generate the Fig. 4(a) profile with the exception of the initial flow-rate (prior to flow splitting) being 0.1 ml/min (1.0 μl/min). Human plasma injection is 2.5 μl diluted sample (1/10, v/v plasma/A′) and 50 μl diluted sample (1/10, v/v plasma/A) in the respective cases (1D, 2D).

2.4.2. Two-dimensional separations

Loading of the LiChrospher® 60 XDS (SO_3H/Diol) 25 μm column is performed with A′ (0.01 M potassium phosphate pH 3.0) over 20 min at a flow-rate of 0.1 ml/min during which time the large and (charge-dependent) non-retained sample components are directed to waste. Elution of the target molecules then occurs by means of desorption via decreasing the binding energies of the analytes. Modulation of the binding energies of the species present in the system with the chromatographic surface is achieved by introducing and increasing sodium chloride concentration over time in the elution buffer. The gradient from A′ → B′ (A′ + 1.5 M NaCl) is executed over 40 min at a flow-rate of 0.2 ml/min. First dimension targets after advancing to the second dimension are distinguished with analyte status by deposition on the Chromolith® CapRod® RP-18 endcapped 300–0.1 mm column. Solvent exchange on the second dimension is monitored by pressure gauge in this dimension and the profiles are recorded once the predetermined value for A″ is leveled. The 2D profiles in Figs. 5–7 are generated accordingly.

2.4.3. Column switching

In valve position A (Fig. 1) the matrix, large sample components and non-interactive sample constituents are directed to waste while the interacting species (target molecules) experience enrichment on the internal surface of the LiChrospher® 60 XDS (SO_3H/Diol) 25 μm. In valve position B (Fig. 1) the target molecules are transferred to the second dimension column where – by 'surviving' the flow splitter – they are promoted to analytes and separated (in valve position A). Fractionated target transfer from the first to the second dimension separation compartment is – although possible – not performed, hence, the documented platform may more accurately be termed a separation system with integrated on-line sample clean-up rather than a two-dimensional separation formation. Heart-cutting or comprehensive sample fractionation is, however, feasible with the penalty of increased time expenditure looming.

2.4.4. Chromatographic conditions

All presented profiles are separations acquired on the Chromolith® CapRod® RP-18 endcapped 300–0.1 mm column. Preceding on-line and off-line raw-data are not shown. In the case of the on-line hyphenated systems, the first dimension data information is lost due to the platform set-up and human serum albumin (HSA) depletion on the off-line affinity column is carried out according to established affinity chromatographic procedures [42,43].

The operation of LiChrospher® 60 XDS (SO_3H/Diol) 25 μm columns for sample clean-up requires a loading buffer (A′) and an elution buffer (B′). Loading the sample was performed with 0.01 M, pH 3.0 potassium phosphate at a flow-rate of 0.1 ml/min. Elution occurred with buffer B′ (B′ = A′ + 1.5 M NaCl) at a flow-rate of 0.2 ml/min.

Irrespective of one or two-dimensional separations, the flow-rate prior to flow splitting was 0.1 and 0.2 ml/min for the Chromolith® CapRod® RP-18 endcapped 300–0.1 mm (cf. figure captions). The flow-rate after the passive split varies accordingly in the range between 1.0 and 2.0 μl/min (determined by water gravimetry under standard conditions). Loading was either by transfer of the retained fraction from the first dimension or by injection from the auto-sampler through the six-port valve [41]. Eluents may feature background electrolytes (BE) and CH_3CN/water based mobile phases with or without TFA modulation.

The affinity column was loaded at 0.05 ml/min loading buffer, washed with 10 column volumes of binding buffer at

1 ml/min and eluted with five column volumes elution buffer also at 1 ml/min.

All experiments were performed in ambient temperature and monitoring of the presented profiles occurred at a UV detection wavelength of 214 nm.

2.5. Chemicals and reagents

The solvents, buffer salts, salts and thiourea and other reagents such as ortho-phosphoric acid 85% and TFA were provided by Merck, KGaA, Darmstadt, Germany and were of gradient grade purity, p.a., and for spectroscopy quality, respectively. The organic modifier utilised in these investigations was CH_3CN. The buffers were prepared as 100 mM stock solutions from the respective salts and acids to yield the desired pH. The BE was prepared by mixing the organic modulator and the buffer to result in the desired phase ratio (monolithic dimension). The eluents were prepared by dissolving the buffer salt and adjusting the pH and molarity (A′) and adding NaCl (B′) (RAM dimension). Sonication occurred in a Bandelin Sonorex TK 52, Berlin, Germany to ensure appropriate degassing of the BE prior to dosage and utilisation. Water was deionised and purified utilising a MilliQ-system by Millipore, Eschborn, Germany.

3. Results and discussion

The separation platform utilised to acquire the human hemofiltrate and plasma profiles presented below consists of an on-line sample preparation step in the first dimension and an orthogonal separation mode in the second dimension. A peculiarity of the system is that the elution from the second dimension may be electrically assisted introducing complementary temperament to the profiles obtained by applying different operational modes in the second dimension(s) of the total analysis system. The novelty instrumentalised here is application of time-variant electric fields simultaneously with the more prominent solvent strength gradients to generate the profiles off the second dimension. Consequently, electric potential gradient generation is not limited to fixed polarity but may be applied across zero potential to tune selectivity.

3.1. Fundamentals

Some basic considerations on the transport phenomena occurring in the monolithic (electro)chromatographic separation system are detailed in the subsequent sections. The effects generated by superimposed flow regimes in particular and their influence on the separation are presented together with the utilised system parameters and the resulting potential gradients.

3.1.1. Single analyte analysis

Additionally to the persuasive data sampled to prove the feasibility of electric field and dynamic electric field assisted multi-dimensional LC, investigative series of measurements into fundamental principles presented in Fig. 2 have been undertaken. The presented platform resembles first and foremost LC equipment and, hence, the hydrodynamic pressure differential is the dominant driving force of the flow regime for the generated chromatograms while electrically-driven flow compliments the velocity of the pressure-driven flow when the applied potential is positive (corresponding to a negative applied potential gradient) and hinders the pressure-driven flow when the applied potential is negative (corresponding to a positive applied potential gradient). Variations in the appearance of the chromatograms are consequently limited to electrically driven alterations within this regime. By evaluating the deviations in the chromatographic behaviour of the unretained compound thiourea in response to the prevailing pressure, comfort zones for flow-rate and electric field generation may be determined. The Fig. 2A plot displays the elution time versus the system immanent voltage. Since low pressure corresponds to proportionally humble hydrodynamic flow, it is apparent from the slope of the retention time versus applied voltage that the electric field contribution to the elution time is of greater influence and, accordingly, enhances the effect with respect to achievable profile modification at small flow-rates as compared to larger ones. The accomplishable elution time discrimination is exorbitant given that a non-interactive substance is (electro)chromatographed. In Fig. 2B, plates/capillary are plotted versus applied voltage. As before, the flow regime is evident evaluating the efficiency under the influence of applied electric fields. Very high flow-rates are detrimental to the column efficiency and under favourable electric field conditions

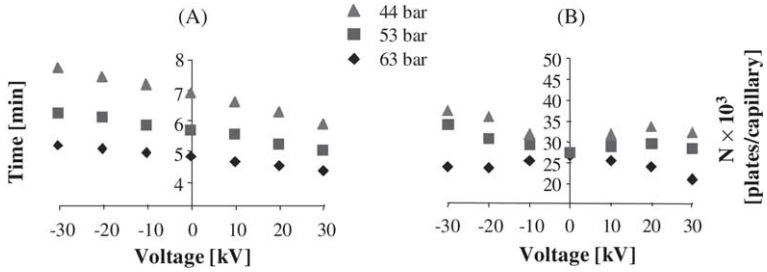

Fig. 2. (Electro)chromatographic thiourea conduct under different back-pressure conditions on Chromolith® CapRod® RP-18 endcapped 300–0.1 mm, (A) elution time vs. (applied) voltage plot, (B) efficiency vs. (applied) voltage plot.

(when the direction of the EOF compliments the direction of the pressure-driven flow) the loss of column efficiency at the higher applied pressures becomes significant as characteristic times for mass transfer along the length of the column in the macropores begin to diverge significantly from the characteristic time for mass transfer in the mesoporous skeleton even if electroosmotic flow could be generated in the mesopores. At the lower applied pressures where the overall flow-rate is lower and closer to the flow-rate of maximum efficiency (the flow-rate where the minimum in the plate height versus flow-rate curve occurs), under favourable electric field conditions the added benefit of electroosmotic flow in the mesopores could contribute to increasing column efficiency but applying increasing voltages results in inflicting accumulating damage to the efficiency since the time constant for mass transfer in the macropores eventually begins to diverge from the time constant for mass transfer in the mesopores as the flow-rate in the macropores increases more significantly at higher voltages than the flow-rate in the mesopores. Under unfavourable electric field conditions (when the applied voltage is negative resulting in a positive voltage gradient and electrically-driven flow hinders the overall flow-rate) column efficiency can be increased for the lower applied pressures as the flow-rate decreases towards the flow-rate of maximum efficiency where mass transfer resistance due to oppositely directed electroosmotic flow in the mesopores is not yet significant, yet as the applied pressure increases and the overall flow-rate increases far above the flow-rate of maximum efficiency, the mass transfer resistance in the mesopores due to the possible reverse directed electroosmotic flow has an increasingly detrimental effect on the column efficiency.

3.1.2. Complex sample analysis

These findings are – visiting Figs. 3, 4, 6 and 7 – likewise manifested in the multi-component (dynamic) electrically assisted LC (Figs. 3, 4, 6(1D) and 7(1D)) and electrically assisted integrated sample clean-up two-dimensional LC profiles (Figs. 6(2D) and 7(2D)). In Figs. 3(d) and 4(e) the time-variant electric field is schematically designated by the intersecting guides with the horizontal line indicative of opposite polarity on either side. While the separation in Fig. 3(d) is obtained at larger flow with the effects on selectivity and efficiency appearing to be subcritical incidents, the relationship of flow-rate and time-variant electric field is not only more prosperous but promising in the Fig. 4(e) application. A multi-component peak is straightforwardly fractionised. The electrokinetic system set-up is chosen to accelerate positively charged analytes and decelerate negatively charged analytes and upon reversal of polarity to reverse their respective electrokinetic migration velocity vector to further enhance theses migrational effects on charged probes. By scrutinising the chromatographic conditions (Section 2, figure captions) it is evident that with the exception of Figs. 3 and 6(1D) principally all analytes bear positive charge. In this light, it is obvious that the effect of running the two-pronged gradient attack for analyte displacement is particularly successful giving complex analytical problems a work-over. The following beneficial consequences apply upon conducting the two-fold gradient elution. Early and late eluting analytes experience the largest fields and hence are resolved with very high efficiency. On either side of the reversal of polarity the electrokinetic migration velocity vector changes and fosters resolution of closely or co-eluting probes. By selecting appropriate (electro)chromatographic conditions or suitable on-line/off-line chromatographic dimensions the analytes may be charged to support comprehensive exploitation of the available acceleration/deceleration potential. Zone sharpening effects as a consequence of the prevailing electric field in the mobile phase and more prominent on the chromatographic surface are believed to be operative throughout the duration of the entire separation.

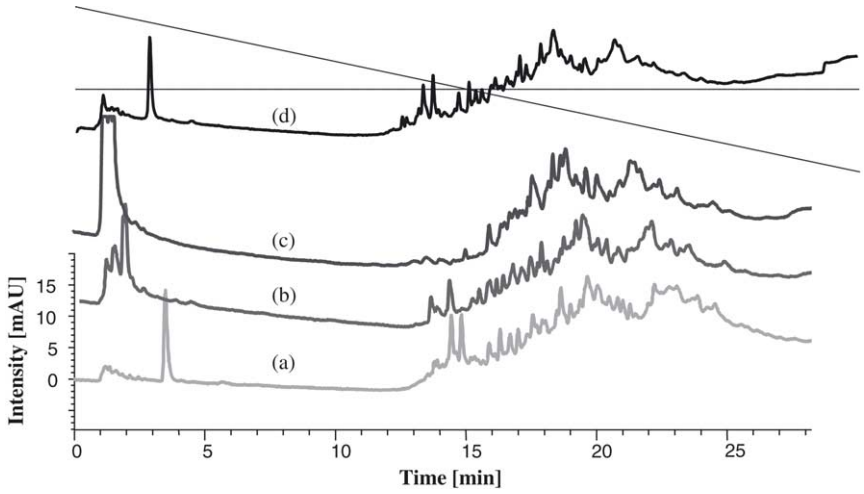

Fig. 3. Separation of 10 μl (10 mg/ml) human hemofiltrate on the Chromolith® CapRod® RP-18 endcapped 300–0.1 mm, LC gradient A″ → B″ in 30 min at 0.2 ml/min (2.0 μl/min), (time-variant) voltage gradient (a) 0 kV, (b) +20 kV, (c) −20 kV, (d) +20 kV → −20 kV (reversal of polarity (r.o.p.) at 15 min).

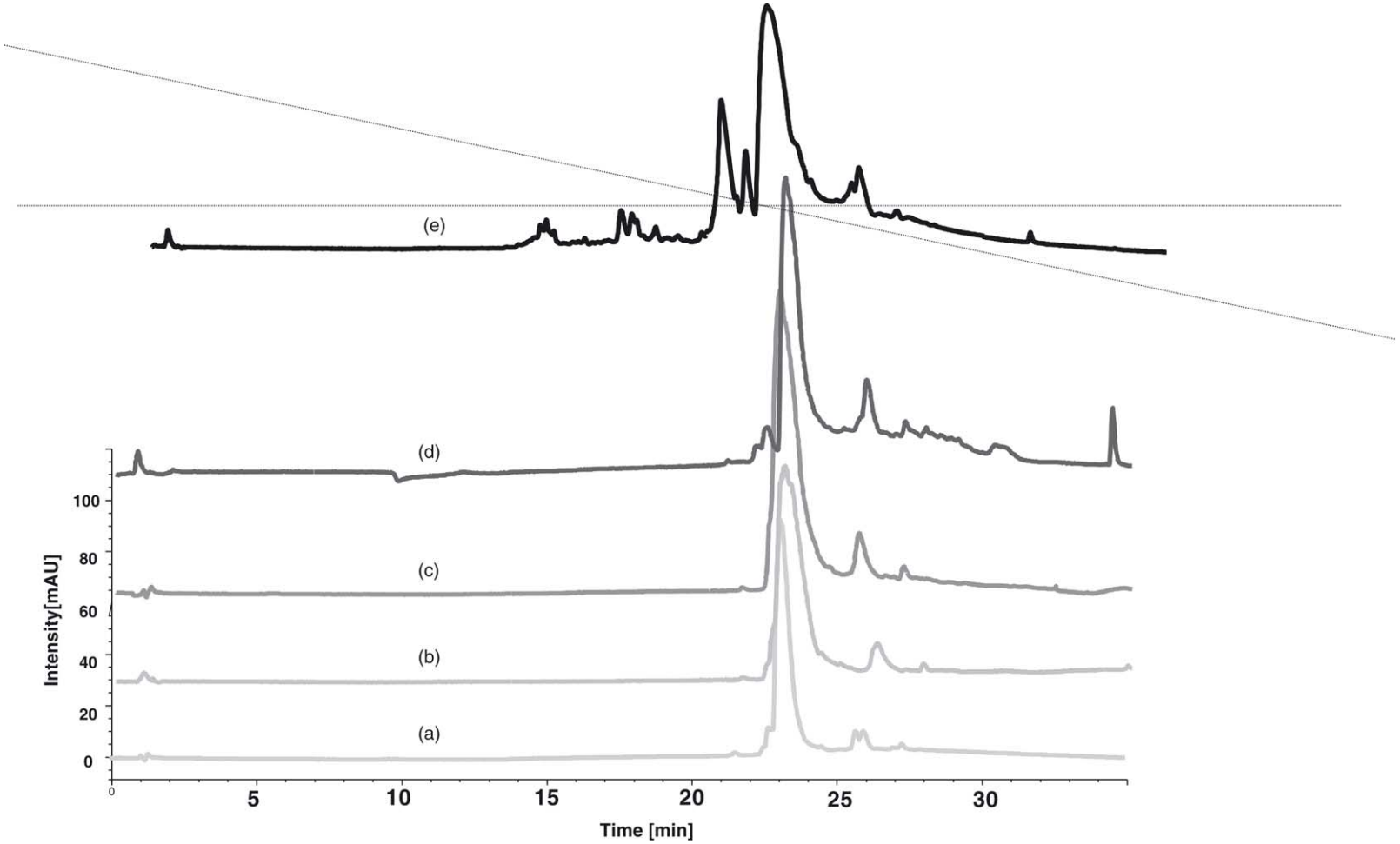

Fig. 4. Separation of 10 μl (1/10, v/v plasma/A″) human plasma on Chromolith® CapRod® RP-18 endcapped 300–0.1 mm, LC gradient A″ → B″ in 46 min at 0.2 ml/min (1.5 μl/min), (time-variant) voltage gradient (a) 0 kV, (b) +20 kV, (c) −20 kV, (d) +20 kV → −20 kV (r.o.p. at 23 min), (e) +30 kV → −30 kV (r.o.p. at 23 min).

3.2. One-dimensional separations

In Fig. 3, some subtle variations with respect to selectivity features of the hemofiltrate profiles are evident in response to the electric fields applied during the entire term of the progression of the hydrodynamic gradient elution. In particular, the peak distribution within the elution window is object to change (Fig. 3(a)–(d)). For the results presented in Fig. 3, the pH of the solution is 7.5 which provides a significant negative charge on the surface of the Chromolith® CapRod® RP-18 endcapped 300–0.1 mm monolith while the relatively low ionic strength of 5 mM provides a significantly large thickness of the electrical double layer (Debye length) and, thus, the zeta potential at the adsorptive surface should have a significantly large negative value [26–28]. Consequently, the application of the electric field in Fig. 3(b)–(d) will have a significant effect, not only on the magnitude of the electrophoretic mass fluxes of the charged sample constituents along the axial direction, x, of the monolith, but also on the magnitude of the electrically-driven flow that is simultaneously occurring with the more dominant pressure-driven flow. The temporally constant potential of +20 kV applied to the monolith (Fig. 3(b)) results in a negative applied electric potential gradient along the length of the monolith ($dV/dx < 0$) and, thus, the electrophoretic mass flux of positively charged sample constituents is directed along the positive axial direction, x, of the monolith as well as the direction of the electrically-driven flow while the electrophoretic mass flux of the negatively charged sample constituents is directed against the net direction of mass transfer. Consequently, the overall flow-rate in the macropores of the monolith will increase slightly as the electrically-driven flow is complimentary to the pressure-driven flow, pure electroosmotic flow along the positive axial direction, x, could be generated in the mesopores of the monolithic skeleton which decreases mass transfer resistance of all sample constituents in the mesoporous structure. Furthermore, due to the mechanism of electrophoretic migration, the transport rate of positively charged sample constituents will increase along the direction of net mass transfer relative to the magnitude of their charge/mass ratio while the transport rate of the negatively charged components along the direction of net mass transport will decrease relative to the magnitude of their charge/mass ratio. Of course, the elution times of the sample constituents depends not only on the overall mass transport rate (combination of diffusion, electromigration, and convective mass transfer), but also on their relative adsorption affinities. However, it is clear that the mechanisms of mass transfer (electrophoretic migration and electroosmotic flow) brought about by the application of the potential difference along the length of the monolith provides an additional means of separation by exploiting the differences in the charge/mass ratio of the sample constituents as well as possibly decreasing the mass transfer resistance in the mesopores. For the chromatogram presented in Fig. 3(c), the applied potential of −20 kV provides a positively valued potential gradient along the axial direction, x, of the monolith and, thus, the behaviour of the electrophoretic mass fluxes of the sample constituents will be opposite to those discussed for Fig. 3(b) while the electrically-driven flow in the system is directed opposite to the net direction of mass transfer and acts to slow down the net flow in the column. If electroosmotic flow is generated in the mesopores of the monolith, then the oppositely directed (with respect to the net direction of mass transfer) magnitude of this flow could result in an increase in the mass transfer resistance in the mesopores. The novel case presented in Fig. 3(d) for the dynamic applied potential provides the benefit of having accelerated electrophoretic mass transfer rates for both positively charged and negatively charged sample components at different periods of time during the analysis [44]. At early times, the mass transport rates of the positively charged species are significantly accelerated (along with the rate of fluid flow) and, as time progresses and the sign of the applied potential switches from positive to negative, the mass transfer rates by electromigration of the negatively charged analytes are enhanced.

The response in view of the raw-data to the various applied electric field conditions is superiorly monitored in Fig. 4 with the paramount separation achieved by exploiting the full range electric potential gradient at the high voltage supply's disposal – including reversal of polarity (Fig. 4(e)). It should be noted that the electrically assisted tuning of the predominantly hydrodynamically driven separation spares the presence of a buffer in the eluent [45]. For the results presented in Fig. 4, the pH of the solution is very close to the point of zero charge for C-18e modified silica surfaces [46,47] and, thus, the magnitude of the electrically-driven flow should be, for all practical purposes, negligible for all chromatograms involving an applied potential along the length of the column (Fig. 4(b)–(e)). Therefore, the benefits for separation obtained by applying a potential difference along the length of the column are attributed to electrophoretic migration of the charged components. The results presented in Figs. 3(d) and 4(e) suggest that the dynamic applied electric field strength could act to significantly enhance the separation of charged components based on their charge/mass ratio, with positively charged components having a larger charge/mass ratio eluting earlier when the overall range of the applied potential difference is largest (Fig. 4(e)) and also decreasing the elution times of the negatively charged components when the overall range of the dynamic applied potential difference is largest (Fig. 4(e)).

3.3. Two-dimensional separations

With these extraordinary separations acquired on a one-dimensional system in hand, hyphenation with a sample complexity reducing module preferably to yield an on-line platform emerges as an obvious desire. In Fig. 5, the human hemofiltrate sample serves as a gauge for a successful on-line sample clean-up strategy in the conventional format (hydrodynamic drive). The sample is both desalted and liberated from (i) sample constituents beyond the cut-off of the hydro-

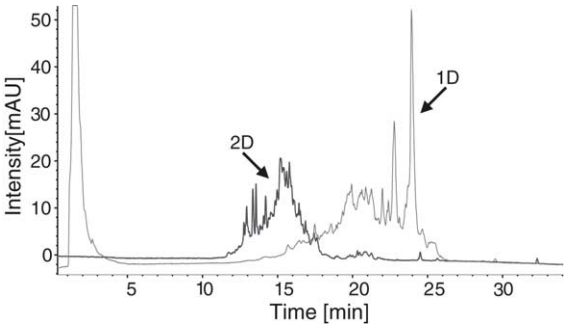

Fig. 5. 1D separation of 10 μl (10 mg/ml) human hemofiltrate on Chromolith® CapRod® RP-18 endcapped 300–0.1 mm, LC gradient A″ → B″ in 30 min at 0.1 ml/min (1.5 μl/min), 2D separation of 10 μl (10 mg/ml) human hemofiltrate on LiChrospher® 60 XDS (SO_3H/Diol) 25 μm, loading with A′ in 20 min at 0.1 ml/min, LC gradient A′ → B′ in 40 min at 0.2 ml/min, on-line hyphenated with Chromolith® CapRod® RP-18 endcapped 300–0.1 mm, LC gradient A″ → B″ in 30 min at 0.1 ml/min (1.5 μl/min).

dynamic size exclusion limit and (ii) those bearing a negative charge, prior to the transfer to the second dimension. Some additional remarks appear to be justified to facilitate the perception of the figure trends. Firstly, the single dimension (1D) and corresponding hyphenated (2D) system display different dwell volumes resulting in varying gradient delays. The omission of the autosampler/injector as part of the 1D apparatus results in decreased retention times in the second dimension of the hyphenated platform. Secondly, sample depletion is monitored by absence of sample constituents and target enrichment by zone sharpening, respectively. Thirdly, solvent exchange and non-interactive species are not recorded in the second dimension as data collection is not initiated until baseline stability delivering mobile phase A″ is obtained.

As is evident from Fig. 6 analysis, the hemofiltrate profile may be principally improved by performing the separation time-variant electrically assisted in a BE with acknowledged buffer capacity. The effect of the applied dynamic electric field is documented in the improved peak distribution ob-

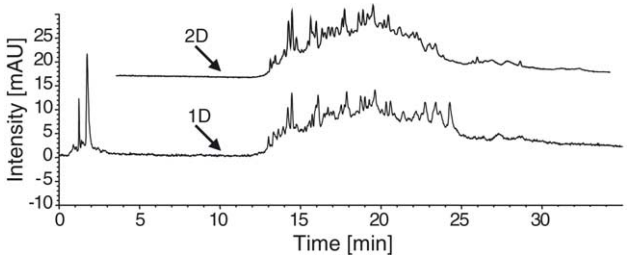

Fig. 6. 1D separation of 10 μl (10 mg/ml) human hemofiltrate on Chromolith® CapRod® RP-18 endcapped 300–0.1 mm, LC gradient A″ → B″ in 30 min at 0.1 ml/min (1.5 μl/min), time-variant voltage gradient +20 kV → −20 kV (r.o.p. at 15 min), 2D separation of 10 μl (10 mg/ml) human hemofiltrate on LiChrospher® 60 XDS (SO_3H/Diol) 25 μm, loading with A′ in 20 min at 0.1 ml/min, LC gradient A′ → B′ in 40 min at 0.2 ml/min, on-line hyphenated with Chromolith® CapRod® RP-18 endcapped 300–0.1 mm, LC gradient A″ → B″ in 30 min at 0.1 ml/min (1.5 μl/min), time-variant voltage gradient +20 kV → −20 kV (r.o.p. at 15 min).

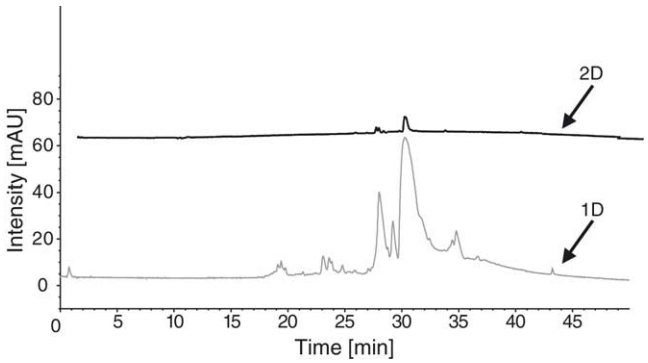

Fig. 7. 1D separation of 10 μl (1/10, v/v plasma/A′) human plasma on Chromolith® CapRod® RP-18 endcapped 300–0.1 mm, LC gradient A″ → B″ in 46 min at 0.1 ml/min (1.5 μl/min), time-variant voltage gradient +30 kV → −30 kV (r.o.p. at 23 min), 2D separation of 10 μl (1/10, v/v plasma/A′) human plasma on LiChrospher® 60 XDS (SO_3H/Diol) 25 μm, loading with A′ in 20 min at 0.1 ml/min, LC gradient A′ → B′ in 40 min at 0.2 ml/min, on-line hyphenated with Chromolith® CapRod® RP-18 endcapped 300–0.1 mm, LC gradient A″ → B″ in 46 min at 0.1 ml/min (1.5 μl/min), time-variant voltage gradient +30 kV → −30 kV (r.o.p. at 23 min).

tained in the profiles with larger separation space. Apart from the obvious analytical discrepancies between Figs. 5 and 6 (cf. figure captions), the two-dimensional profile has been relocated for the convenience of facilitated comparison. Again the sample in the two-dimensional system is significantly reduced in its complexity (given that hemofiltrate is a processed sample per se). Importantly, the analytes display no conspicuity with respect to the peak distribution as a consequence of the sample clean-up procedure [11,48]. Baseline separation in the second dimension of analyte fractions from the second dimension appear to be feasible.

Fig. 7 displays a major handicap of the documented separation platform. It is beyond controversy that the separation hardware is orthogonal with respect to the exploited separation mode, the compatibility of the dimensions of the first and second separation dimension columns, however, is debatable. The target transfer is performed via a passive splitter and therefore the detection sensitivity does not allow conclusive evaluation (this and other limitations of passive flow splitting are discussed in reference [41]). Regarding the mode of detection plasma analysis on the separation platform presented here clearly demands hyphenation with mass sensitive detection in particular bearing the abundance ratios of the prevailing analytes in mind. The removal of high MW sample components is obviously successful while the detection of low MW analytes may suffer from insufficient concentration LODs.

Further separation and detection modes may easily be integrated to gain yet more potent separation tools. An example of an off-line affinity HSA depletion sample preparation step prior to one-dimensional separation (with pure hydrodynamic drive) on named platform is detailed versus the profile of the untreated sample in Fig. 8. The insert shows a similar result obtained by 1D-SDS-PAGE and visualized by

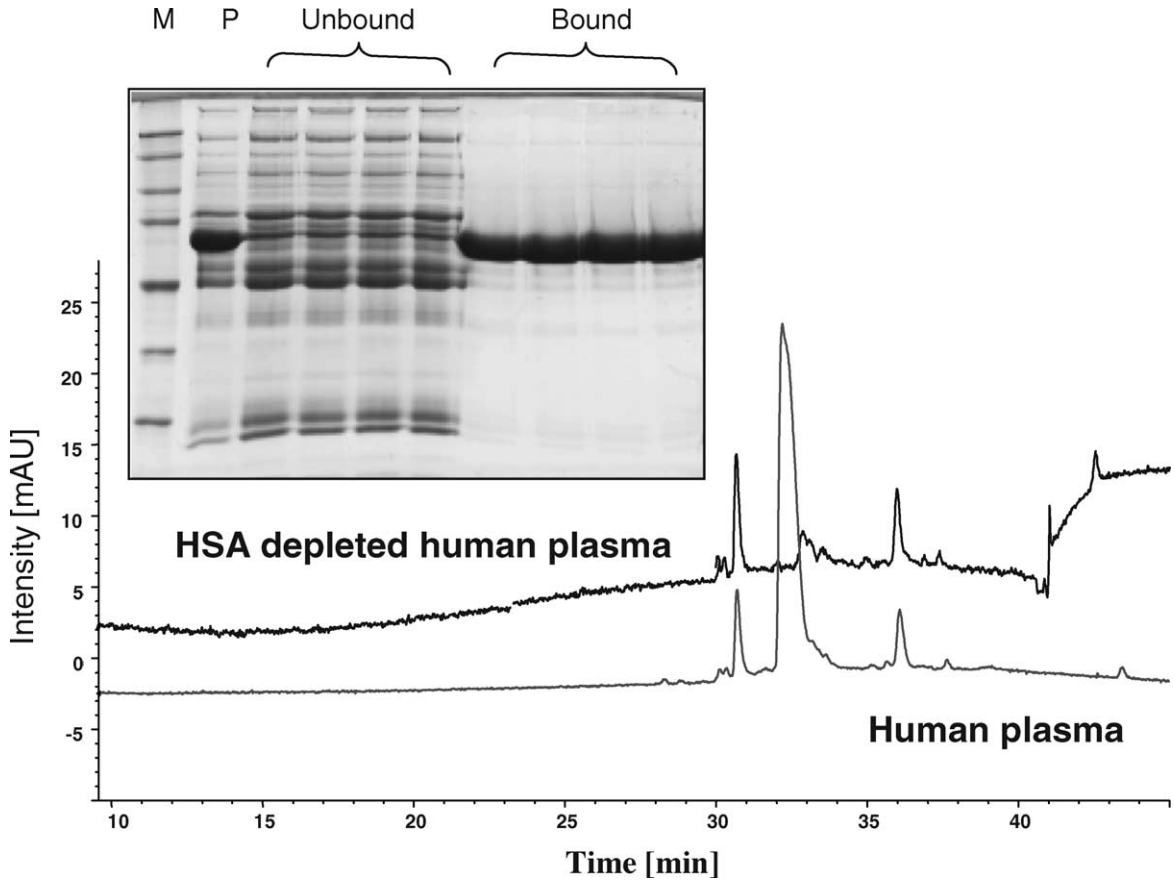

Fig. 8. Separation of 2.5 μl (1/10, v/v plasma/A′) human plasma on Chromolith® CapRod® RP-18 endcapped 300–0.1 mm, LC gradient A″ → B″ in 46 min at 0.1 ml/min (1.0 μl/min), separation of 10 μl (1/10, v/v plasma/A) human plasma on the HSA depletion column, off-line (collected and reintroduced to) Chromolith® CapRod® RP-18 endcapped 300-0.1 mm, LC gradient A″ → B″ in 46 min at 0.1 ml/min (1.0 μl/min). Insert: 35 μl human plasma was processed using the ProteoExtract™ HSA removal column according to the manufacturers instructions. 15 μg protein of each fraction were separated by 1D-SDS-PAGE and visualized by Coomassie® staining. M: molecular weight marker. P: crude human plasma. Unbound: HSA depleted plasma. Bound: HSA and non-specific bound proteins.

Coomassie® staining. The human plasma UV trace in Fig. 8 corresponds to the gel lane P and the HSA depleted human plasma chromatogram represents the unbound fractions, respectively. The total injection amount for the generation of the HSA depleted human plasma profile was calculated based on the elution volume of the unbound fraction from the affinity column and on the assumption of 100% recovery of the sample constituents from that particular fraction of the original sample. The HSA depleted plasma profile displays all afore mentioned benefits of a successful sample clean-up procedure.

4. Conclusions

Samples from biological matrices represent a major challenge to the scientists involved in physical and chemical analysis with respect to their complexity (number of constituents) and composition (abundance ratio of constituents). Contemporary approaches are therefore frequently developed in view of an analytical problem rather than a particular sample with the labour of separation optimisation remaining a task indeed associated with the individual analysis.

The electrically assisted liquid chromatographic separation of biological samples is enriched with the dynamic electric field superimposition on hydrodynamic flow to realise analysis and moreover with the facet of polarity reversal during the analysis. The potential of enhancing resolution and peak distribution together with creating aggrandised separation space may be exploited to advance analysis of complex sample mixtures. Integrated on-line sample clean-up multidimensional separations provide the key to reduce the inconveniences associated with sample handling, target transfer, analyte–matrix interactions and abundance ratios of individual analytes.

The first dimension cation exchange is the ideal supplement to the portrayed dynamic electric field separation in the second dimension since negatively charged sample components are omitted from the first dimension analysis. The voltage gradient is chiefly designed to enlarge the separation space for positively charged analytes and to enhance their resolution within this expanded separation space. However,

separations of negatively charged species may be accomplished in equally remarkable fashion by simply operating anion exchange in the first dimension and reversing the electric potential gradient in the second dimension because then negatively charged analytes should experience sophisticated resolution in the negative charge bearing analyte specific inflated separation space.

The presented separation conditions for all acquired biological sample profiles indicate operation of (dynamic) electric potential and eluotropic strength gradients in tandem and simultaneously although separation tuning in the second dimension may be performed decoupled (independently time-variant) to achieve a desired analytical goal.

References

[1] H.J. Issaq, Electrophoresis 22 (2001) 3629.
[2] F.M. Lanças, J. Braz. Chem. Soc. 14 (2003) 183.
[3] S.D. Patterson, Curr. Opin. Biotechnol. 11 (2000) 413.
[4] H. Wang, S. Hanash, J. Chromatogr. B 787 (2003) 11.
[5] P.A. Haynes, J.R.I. Yates, Yeast 17 (2000) 81.
[6] I. Lefkovits, J. Chromatogr. B 787 (2003) 1.
[7] T. Laurell, G. Marko-Varga, Proteomics 2 (2002) 345.
[8] K.E. Neet, J.C. Lee, Mol. Cell. Proteomics 1 (2002) 415.
[9] S.D. Patterson, R.H. Aebersold, Nat. Genet. 33 (2003) 311.
[10] B. Seliger, R. Kellner, Proteomics 2 (2002) 1641.
[11] W.S. Hancock, S.L. Wu, R.R. Stanley, E.A. Gombocz, Trends Biotechnol. 20 (2002) 39.
[12] W. Naidong, R.H. Pullen, R.F. Arrendale, J.J. Brennan, J.D. Hulse, J.W. Lee, J. Pharma. Biomed. Anal. 14 (1996) 325.
[13] A. Guttman, M. Varoglu, J. Khandurina, Drug Discov. Today 9 (2004) 136.
[14] G.M. Janini, T.P. Conrads, T.D. Veenstra, H.J. Issaq, J. Chromatogr. B 787 (2003) 43.
[15] T.J. Griffin, R. Aebersold, J. Biol. Chem. 276 (2001) 45497.
[16] O. Willemsen, E. Machtejevas, K.K. Unger, J. Chromatogr. A 1025 (2004) 209.
[17] K. Wagner, T. Miliotis, G. Marko-Varga, R. Bischoff, K.K. Unger, Anal. Chem. 74 (2002) 809.
[18] M.P. Henry, Retention Times (CaSSS) XIII (2004).
[19] V. Kahle, M. Vàzlerovà, T. Welsch, J. Chromatogr. A 990 (2003) 3.
[20] A.S. Lister, C.A. Rimmer, J.D. Dorsey, J. Chromatogr. A 828 (1998) 105.
[21] C.A. Rimmer, S.M. Piraino, J.D. Dorsey, J. Chromatogr. A 887 (2000) 115.
[22] M.R. Taylor, P. Teale, J. Chromatogr. A 768 (1997) 89.
[23] W. Zhang, L. Zhang, G. Ping, Y. Zhang, A. Kettrup, J. Chromatogr. A 922 (2001) 277.
[24] F. Steiner, B. Scherer, J. Chromatogr. A 887 (2000) 55.
[25] M. Riekkola, J.A. Jönsson, in: International Union of Pure and Applied Chemistry, 2002, p. 1.
[26] B.A. Grimes, A.I. Liapis, J. Colloid Interface Sci. 234 (2001) 223.
[27] B.A. Grimes, A.I. Liapis, J. Chromatogr. A 919 (2001) 157.
[28] A.I. Liapis, B.A. Grimes, K. Lacki, I. Neretnieks, J. Chromatogr. A 921 (2001) 135.
[29] R. Xiang, C. Horvath, Anal. Chem. 74 (2002) 762.
[30] K.K. Unger, M. Huber, K. Walhagen, T.P. Hennessy, M.T.W. Hearn, Anal. Chem. 74 (2002) 200A.
[31] D. Perett, Ann. Clin. Biochem. 36 (1999) 133.
[32] C.M. Surman, The Use of Capillary Electrophoresis in Proteomics, GE Global Research, 2002.
[33] A. Technologies, Optimizing the Agilent 1100 series LC system: solution guide, Agilent Technologies, 2001.
[34] W.-C. Lee, K.H. Lee, Anal. Biochem. 324 (2004) 1.
[35] G. Choudhary, W. Hancock, K. Witt, G. Rozing, A. Torres-Duarte, W. Irving, J. Chromatogr. A 857 (1999) 183.
[36] K. Walhagen, K.K. Unger, M.T. Hearn, Anal. Chem. 73 (2001) 4924.
[37] K. Wagner, K. Racaityte, K.K. Unger, T. Miliotis, L.E. Edholm, R. Bischoff, G. Marko-Varga, J. Chromatogr. A 893 (2000) 293.
[38] K. Racaityte, E.S.M. Lutz, K.K. Unger, D. Lubda, K.S. Boos, J. Chromatogr. A 890 (2000) 135.
[39] B. Barroso, D. Lubda, R. Bischoff, J. Proteome Res. 2 (2003) 633.
[40] V.V. Tolstikov, A. Lommen, K. Nakanishi, N. Tanaka, O. Fiehn, Anal. Chem. 75 (2003) 6737.
[41] G. Rozing, M. Serwe, B. Glatz, Am. Lab. (2001) 26.
[42] W.C. Lee, K.H. Lee, Anal. Biochem. 324 (2004) 1.
[43] Product Information, ProteoExtract Albumin Removal Kit, CALBIOCHEM.
[44] T.P. Hennessy, R.I. Boysen, D. Lubda, K.K. Unger, M.T.W. Hearn, Procedings of the 27th International Symposium on High Performance Liquid Phase Separations and Related Techniques, Nice, France, 2003.
[45] T. Adam, K.K. Unger, J. Chromatogr. A 89 (2000) 241.
[46] A.N. Heyrman, R.A. Henry, Keystone—Technical Bulletin 99-06 (1999) 1.
[47] R.K. Iler, The Chemistry of Silica: Solubility, Polymerization, Colloid and Surface Properties and Biochemistry of Silica, Wiley Interscience, Hoboken, New Jersey, 1979.
[48] D.V. McCalley, Anal. Chem. 75 (2003) 3404.